



Research paper

Broadband dielectric spectroscopy as an experimental alternative to calorimetric determination of the solubility of drugs into polymer matrix: Case of flutamide and various polymeric matrixes

K. Chmiel^{a,b,*}, J. Knapik-Kowalczyk^{a,b}, R. Jachowicz^c, M. Paluch^{a,b}^a Institute of Physics, University of Silesia, ul. 75 Pułku Piechoty 1a, 41-500 Chorzów, Poland^b Silesian Center for Education and Interdisciplinary Research, ul. 75 Pułku Piechoty 1a, 41-500 Chorzów, Poland^c Faculty of Pharmacy, Department of Pharmaceutical Technology and Biopharmaceutics, Jagiellonian University, Medyczna 9, 30-688 Kraków, Poland

ARTICLE INFO

Keywords:

Amorphous solid dispersion
Molecular dynamics
Dielectric spectroscopy
Stability map
Flutamide
Poly vinylacetate
Poly vinylpyrrolidone
Solubility

ABSTRACT

In this paper we determined the solubility limits of the amorphous flutamide within the two different polymeric matrixes – poly vinylpyrrolidone and poly vinylacetate. In order to achieve this goal, series of broadband dielectric spectroscopy measurements were performed. As a result we found that the maximal amount of the drug that can be successfully dissolved within the PVAc (maintaining the non-supersaturated conditions) is equal to 35 wt% of the amorphous solid dispersion system. Interestingly enough similar results, in terms of solubility limits, were achieved utilizing significantly higher amount of the pharmaceutical – 71 wt% – in the PVP matrix. Accordingly, we established the following relationship in the solubility limits of the amorphous flutamide dispersed within examined polymer matrixes: PVP > PVAc. It is worth highlighting that in order to preserve the thermodynamic stability – one of the two contributors to the physical stability – drug loading in the amorphous solid dispersion system should not exceed its solubility limits. Hence, choosing appropriate amount of the polymer addition will determine if obtained system remains physically stable. Subsequently, we presented the “stability maps” for all investigated FL-based ASD systems from which one might predict the stabilization effect exerted by certain amount of polymer.

1. Introduction

Currently, researchers in the pharmaceutical industry are struggling with the very important problem connected with the dissolution-rate limited bioavailability of almost half of the crystalline Active Pharmaceutical Ingredients (APIs) [1–4]. A promising approach that might overcome this problem is to transform a crystalline drug into its amorphous form [5–10]. Amorphous APIs having higher Gibbs free energy as well as greater free enthalpy than any crystalline polymorph are considered as the most soluble form of drug [11–12]. Unfortunately, one should keep in mind that the higher energetic state, which on the one hand is the reason of better solubility of an amorphous APIs, on the other hand, is responsible for their instability [13]. Disordered pharmaceuticals tend to give back the excess of their internal energy, and consequently during manufacturing or storage might revert into their less soluble, but physically more stable crystalline forms [14–16]. Due to re-crystallization propensity of an amorphous APIs, researchers seek to find the most effective way to stabilize them [17–20]. Proven

strategy for inhibiting devitrification of disordered pharmaceuticals is to disperse them into a polymeric carrier [21–23]. For example, Suryanarayanan and co-workers indicated that 4 wt% addition of the poly vinylpyrrolidone (PVP) polymer has the ability to stabilize amorphous ketoconazole drug. Unfortunately, ketoconazole + 4 wt% of PVP system begins to recrystallize after 105 days at 298 K, what has been detected via X-ray diffraction (XRD) [24]. Improvement of the physical stability was also reported by our group in case of other amorphous API – celecoxib – dispersed in PVP polymer. We showed, that by applying 5 wt% of the polymer, one is able to prolong the stability of celecoxib by 4–5 times, when the sample is stored at 295 K [25]. Furthermore, Aso et al. reported that in the case of amorphous nifedipine, 10% PVP addition slows the rate of the recrystallization by a factor of 300 [26]. Taylor and co-authors reported that amorphous felodipine drug might be effectively stabilized by HPMCAS polymer. Stability of such a system has been monitored at 298 K and 93% RH. Performed experiments indicated that at such extremely humid conditions amorphous solid dispersion (ASD) containing 50 wt% of polymer displays first signs of re-

* Corresponding author at: Institute of Physics, University of Silesia, ul. 75 Pułku Piechoty 1a, 41-500 Chorzów, Poland.

E-mail address: krzysztof.chmiel@smcebi.edu.pl (K. Chmiel).<https://doi.org/10.1016/j.ejpb.2019.01.025>

Received 25 July 2018; Received in revised form 27 December 2018; Accepted 25 January 2019

Available online 28 January 2019

0939-6411/ © 2019 Elsevier B.V. All rights reserved.

crystallization approximately after 490 days [27].

Despite the undoubted potential of amorphous solid dispersion, the numbers of products that have made it through the market is still limited. It is caused by the difficulties in predicting time of physical stability of these systems during storage and/or manufacturing conditions. Consequently, such products require additional long-term stability testing before the drugs can be introduced into the market. It is worth highlighting, that there is a way, which might ensure the thermodynamic stability of a drug-polymer formulation. In order to achieve this goal, two main requirements must be met. The first is the possibility to dissolve the drug within the polymer matrix. The second is the need to preserve the concentration below the equilibrium solubility of the drug in the polymer [28–32]. In light of these findings, determination of drug-polymer solubility is a critical parameter when determining the ratio between drug and polymer in the formulation development of an amorphous solid dispersion.

Up to now there are two main experimental approaches to obtain the value of the aforementioned solubility limits – *annealing method* [33] and *recrystallization method* [28]. Both these methods are based on differential scanning calorimetry (DSC) measurements. In the *annealing method* after annealing in precisely determined conditions (e.g. concentration, time and temperature) the presence or absence of residual crystals – API not dissolved in polymeric matrix – is determined by standard DSC measurements. Even though precision in this kind of measurements is very high, the time consumption of each step forced pharmaceutical scientist to look for a different, faster method. As an answer to this urgent need a *recrystallization method* was proposed. This approach consists of 3 main steps: (i) preparation of supersaturated system; (ii) annealing in various temperature ranges (above the glass transition) for a certain amount of time in order to recrystallize the excess amount of the API; (iii) re-scanning of the partially re-crystallized sample and identification of the concentration of the remaining amorphous sample via comparison to Gordon-Taylor (GT) prediction. This method vastly reduces the amount of time needed to obtain the solubility limits of a system.

Because a new, quick and effective method to determine physically stable concentration of ASD is needed in drug industry, we present alternative method for determining solubility limits of drug in a polymeric carrier [34]. Despite the fact that the proposed approach employs a different experimental technique – dielectric spectroscopy, it is similar to the thermal approach used currently (e.g. *recrystallization method*). Additionally, this method allows online monitoring of the changes in concentration occurring during recrystallization from supersaturated drug-polymer solution.

In this paper we continue our studies and examine solubility limits of different flutamide-based ASDs. Our previously used polymer, Kollidon VA64 (PVP/VA), is a co-polymer of N-vinylpyrrolidone (PVP) and vinylacetate (PVAc). Therefore, herein we investigated the related homopolymers, poly(vinyl pyrrolidone) (PVP) and poly(vinyl acetate) (PVAc). The aim was to determine solubility limits of flutamide (FL) in two different polymers to finally assess which polymer is better stabilizer of FL drug (i.e. the amount of polymer required to obtain the same stabilization effect – full stabilization (saturated solution)).

Thermal properties of drug-polymer systems containing different concentrations of FL and PVAc or PVP have been investigated via DSC. On the basis of DSC data, we determined the concentration dependences of the glass transition temperature of FL + PVAc and FL + PVP systems. These plots finally constitute a “stability map”, from which one might predict the stabilization effect exerted by a certain amount of polymer. To find the border – physically stable – concentrations of FL dispersed into the PVAc or PVP, as well as to examine the molecular mobility of the investigated drug-polymer mixtures we measured them by means of broadband dielectric spectroscopy. The results allowed us to quickly assess the minimal amount of the excipient required to fully stabilize FL drug, and consequently determining, which polymer: PVAc, PVP or Kollidon VA64 is the most effective

crystallization inhibitor of the investigated antiandrogen.

2. Materials and methods

2.1. Materials

Flutamide drug of molecular mass $M_w = 276.21 \text{ g mol}^{-1}$ and purity $\geq 99\%$ was purchased from Sigma-Aldrich and used as received. Poly vinylpyrrolidone of molecular mass $M_w = 58\,000 \text{ g mol}^{-1}$ was purchased from Alfa Aesar (Germany, LOT: 10188588) with impurity content equal to 0.01% and used as received. Poly vinylacetate of molecular mass $M_w = 50\,000 \text{ g mol}^{-1}$ was purchased from Alfa Aesar (Germany, LOT: 10196348) with impurity content equal to 0.0001% and used as received.

2.2. Preparation of binary system

The flutamide-based amorphous solid dispersion systems were prepared at different weight concentrations of PVAc and PVP in each sample. To acquire homogeneous samples we mixed compounds with polymer at appropriate ratios in mortar for approximately 20–30 min. Prepared in this way mixtures were then melted at $T = 410 \text{ K}$ – during the first DSC scan – and vitrified – by fast cooling during second DSC scan – in case of calorimetric measurements. Samples preparation for the BDS measurements involved melting at $T = 410 \text{ K}$ followed by vitrification on a previously chilled copper plate. All measurements were performed immediately after preparation of the amorphous systems to avoid recrystallization.

2.3. Differential scanning calorimetry

Thermodynamic properties of FL, Kollidon VA64 and their binary systems were examined using a Mettler-Toledo DSC 1 STARE System. The measuring device was equipped with a HSS8 ceramic sensor having 120 thermocouples. The instrument was calibrated for temperature and enthalpy using indium and zinc standards. Crystallization and melting points were determined as the onset of the peak, whereas the glass transition temperature as the midpoint of the heat capacity increment. The samples were measured in an aluminum crucible (40 μL). All measurements were carried out in range from 260.15 K to 410.15 K with 10 K/min heating rate except for the neat PVP measurements which in order to observe glass transition was carried out up to the 480.15 K.

2.4. Broadband dielectric spectroscopy

The dielectric measurements of FL-based ASDs were carried out using Novo-Control GMBH Alpha dielectric spectrometer, in the frequency range from 10^{-1} Hz to 10^6 Hz at temperatures from 153.15 K to 373.15 K with heating rate equal to 1 K/min. The temperature was controlled by a Quatro temperature controller with temperature stability better than 0.1 K. Dielectric studies of FL and its binary systems were performed immediately after its vitrification by fast cooling of the melt in a parallel-plate cell made of stainless steel (diameter 15 mm, and a 0.1 mm gap with quartz spacers).

3. Results and discussion

3.1. Thermal properties of FL + PVAc mixtures.

Thermal properties of neat components (amorphous FL and PVAc polymer) and their binary amorphous compositions (FL + 6 wt% PVAc, FL + 25 wt% PVAc, FL + 50 wt% PVAc, FL + 65 wt% PVAc and FL + 75 wt% PVAc) have been investigated by means of Differential Scanning Calorimetry. During these studies the samples were heated from 260 K to 410 K with a rate of 10 K/min. The results obtained from

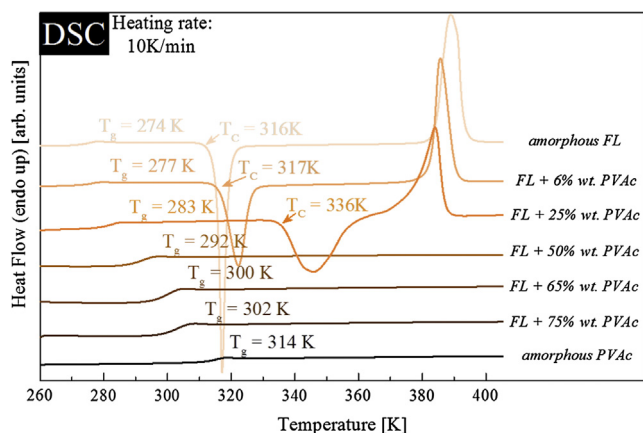


Fig. 1. Thermograms of amorphous: (a) FL (peach), (b) FL + 6 wt% PVAc (mango), (c) FL + 25 wt% PVAc (marigold), (d) FL + 50 wt% PVAc (rust), (e) FL + 65 wt% PVAc (coffee), (f) FL + 75 wt% PVAc (brown) and (g) PVAc (black). (For interpretation of the references to colour in this figure legend, the reader is referred to the web version of this article.)

all these experiments are presented in Fig. 1. As can be seen both: the neat components as well as their mixtures are characterized by a single glass transition event. The temperature of glass transition (T_g) values of neat amorphous FL, neat PVAc polymer, and the mixtures containing: 6, 25, 50, 65 and 75 wt% of PVAc are equal to 274 K, 314 K, 277 K, 283 K, 292 K, 300 K and 302 K, respectively.

It should be noted that the glass transition temperature of the investigated drug-polymer systems grow continuously with increasing the polymer content. This behavior is common and can be caused by one of the following reasons or a combination thereof: (i) the antiplasticization effect exerted by the polymer having 40 K higher glass transition temperature than the neat drug or/and (ii) specific interactions existing between the drug and the polymer. It is worth to recall that, if the antiplasticization effect is dominant, the mixtures T_g should vary with polymer content in accordance to Gordon-Taylor prediction, which is defined as follow:

$$T_g = \frac{W_1 T_{g1} + K W_2 T_{g2}}{W_1 + K W_2} \quad (1)$$

where the T_g , T_{g1} , T_{g2} are the glass transition temperatures of the drug-polymer mixture, the amorphous drug, and the polymer, respectively; W_1 and W_2 are the weight fraction of the drug and polymer and K is a parameter that can be calculated according to the formula:

$$K \approx \frac{\Delta C_{p2}}{\Delta C_{p1}} \quad (2)$$

where ΔC_{p1} and ΔC_{p2} are the changes in heat capacity at T_g of drug and polymer, respectively. In Fig. 2 the experimentally obtained T_g values of the mixtures with different concentration of FL and PVAc (presented as points) have been compared with glass transition temperature values predicted from the Gordon-Taylor equation (marked as dashed line). As can be seen the experimentally obtained T_g s are in perfect agreement with GT prediction. These results suggest that in the studied mixtures there should not be additional drug-polymer interactions.

Referring back to Fig. 1, it is worth to mention that upon further heating of the samples – above T_g – only neat FL and two drug-polymer compositions containing 6 and 25 wt% of the polymer exhibit exothermic event reflecting re-crystallization. Taking into account that the polymeric additive on the one hand shifts the re-crystallization process of FL towards higher temperatures or even eliminates it from the DSC experiment timeframe, and on the other hand it increases the value of FL's glass transition temperature, what is equivalent with slowing down its molecular mobility, one can conclude that PVAc is able to improve physical stability of amorphous form of FL. Nevertheless, based on

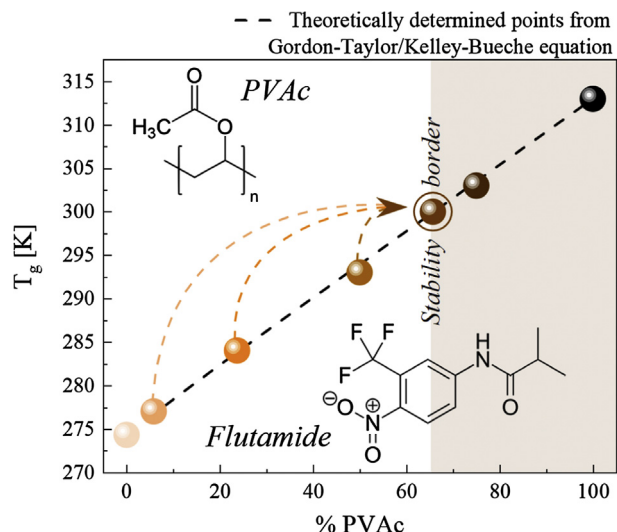


Fig. 2. Glass transition temperatures of FL – PVAc mixtures. Points correspond to the experimentally determined T_g values. The dashed line represents the Gordon-Taylor/Kelley-Bueche equation. The black ring is the point obtained by using T_g related to the $\tau_{\alpha'}$ process (T_g obtain when crystallization ceased). Upper inset shows chemical structure of Polyvinyl acetate while lower corresponds to the structure of Flutamide.

presented data we are not able to determine which concentration of FL + PVAc will be sufficiently stable to introduce this system safely into the market. The fact that sample with 50 wt% of the polymer did not exhibits any tendency towards cold crystallization during the calorimetric measurement performed with the heating rate equal to 10 K/min, does not guarantee that it will be physically stable also during other experiments, e.g. when slower heating rate will be applied.

3.2. Molecular dynamics studies of FL + PVAc mixtures

In our previous paper we, reported, that based on the molecular dynamics studies it is possible to quickly determine the border – physically stable – concentration of ASD. In that particular case, the flutamide-based ASD containing Kollidon VA64 polymer has been investigated [34]. In this section we performed similar – non-isothermal, dielectric – experiments on ASD containing FL, with different than previously used – PVAc – polymeric matrix. The aim of these experiments was to determine solubility limit of FL drug in chosen polymer.

ASD containing FL + 25 wt% of PVAc has been selected as a first candidate for dielectric studies. The reason why we choose this particular concentration is because in order to observe described above transformation, we have to start from supersaturated drug-polymer composition due to the fact that only such system is able to re-crystallize. Taking into account that this specific concentration re-crystallize rather easily, what has been proved by DSC data, we selected it for the further molecular dynamics studies. The representative dielectric loss spectra of FL + 25 wt% PVAc mixture are shown in Fig. 3a. As can be seen dielectric loss spectra recorded at temperature lower than the glass transition temperature of this system did not exhibit any secondary relaxation processes. Herein, only the loss characterized by a power law $\epsilon''(f) = Bf^{-\lambda}$ with $\lambda < 0.2$ might be visible. This feature is usually attributed to nearly constant loss (NCL), which is consider as the manifestation of the cage molecular dynamics. It is worth noting that neat FL as well as FL + Kollidon VA64 ASDs (which were previously measured) exhibit the same features when measured below its T_g s [34]. Spectra of the investigated drug-polymer mixture (FL + 25 wt % PVAc) registered at $T > T_g$ exhibit one well resolved loss peak corresponding to the structural – α – relaxation (see Fig. 2a). Observed peak moves towards higher frequencies with increasing temperature

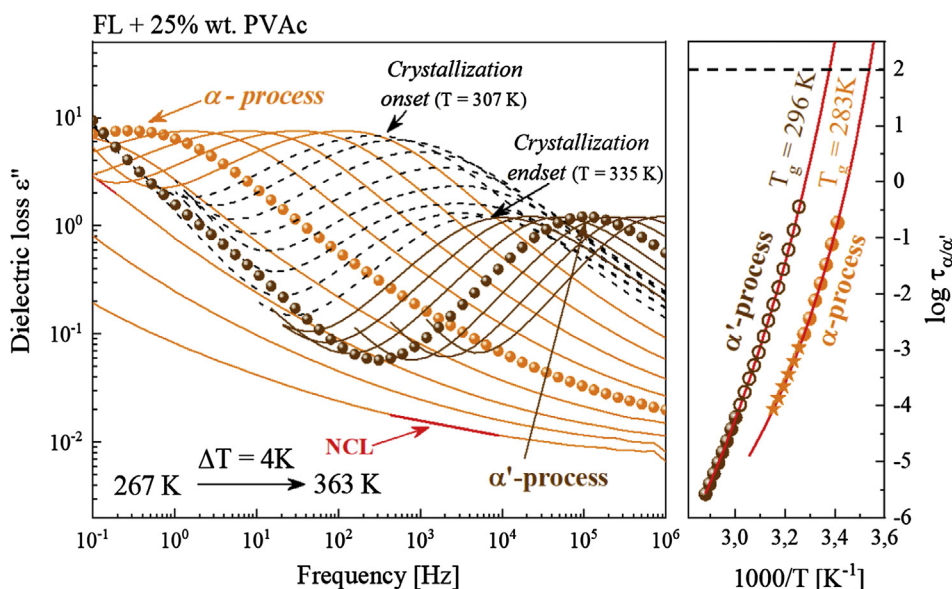


Fig. 3. Left panel presents the dielectric loss spectra of amorphous binary mixture of FL + 25 wt% PVAc. Orange lines indicates the α process, black dashed lines corresponds to the crystallization process and the brown lines represents the additional process. Right panel shows relaxation map of binary mixtures of FL + 25 wt% PVAc as follows τ_{α} (orange circles), crystallization of FL + 25 wt% PVAc (orange stars), $\tau_{\alpha'}$ (brown circles) and $\tau_{\alpha'}$ obtained during cooling (brown open circles). Temperature dependence of τ_{α} and $\tau_{\alpha'}$ in the supercooled liquid has been described by VFT equations (red solid lines). (For interpretation of the references to colour in this figure legend, the reader is referred to the web version of this article.)

and its intensity decrease slightly according to the Langevin formula by a term proportional to $1/T$ up to the $T = 303$ K. Above this temperature the dielectric strength of the α -relaxation ($\Delta\epsilon$) begins to decrease rapidly with temperature, what can be seen on dielectric loss spectra as a drop in the intensity of the structural relaxation peak (see black spectra in Fig. 3a). Taking into account that the dielectric strength ($\Delta\epsilon$) is proportional to the number of units involved in structural relaxation, such a sudden drop in the intensity of structural relaxation reflects the onset of the sample re-crystallization [35]. As Fig. 3a shows the re-crystallization process ceased at $T = 335$ K. What is more, upon further heating the observed peak (remaining after observed re-crystallization of a part of the sample's volume), which we called α' -process, shifts toward higher frequencies and does not display further decrease in intensity, indicating that there was no additional re-crystallization. This result suggests that only the excess of FL re-crystallized from the supersaturated drug-polymer system. Mixture obtained in this way is in fact saturated drug-polymer system (physically stable) and in the same time is characterized by higher than initial polymer concentration. Consequently, by analyzing temperature dependence of α' -relaxation time ($\tau_{\alpha'}(T)$), we should be able to determine border concentration of FL dispersed in PVAc, which will guarantee high physical stability of the system.

To obtain the values of both τ_{α} and $\tau_{\alpha'}$ for FL + 25 wt% PVAc at various temperatures, the dielectric loss spectra were firstly fitted by means of the Havriliak-Negami (HN) function (Eq. (1)): [36]

$$\epsilon^*(\omega) = \epsilon_{\infty} + \frac{\Delta\epsilon}{[1 + (i\omega\tau_{HN})^a]^b} \quad (3)$$

where ϵ_{∞} is high frequency limit permittivity, $\Delta\epsilon$ is dielectric strength, ω is equal to $2\pi f$ (f stands for frequency), τ_{HN} is the HN relaxation time, a and b represents symmetric and asymmetric broadening of relaxation peak. Then, based on the fitting parameters determined above, the values of τ_{α} and $\tau_{\alpha'}$ were calculated from the following formula:

$$\tau_{\alpha/\alpha'} = \tau_{HN} \left[\sin\left(\frac{\pi a}{2 + 2b}\right) \right]^{\frac{1}{a}} \left[\sin\left(\frac{\pi ab}{2 + 2b}\right) \right]^{\frac{1}{a}} \quad (4)$$

Relaxation times obtained from described above fitting procedure are presented in Fig. 3b as a filled orange (in case of the α -process) and brown (in case of the α' -process) circles.

In the supercooled liquid region, the temperature evolution of structural relaxation time usually shows non-Arrhenius like behavior, and follows the Vogel-Fulcher-Tamman (VFT) equation that is defined as follows: [37–39]

$$\tau_{\alpha}(T) = \tau_{\infty} \exp\left(\frac{DT_0}{T - T_0}\right) \quad (5)$$

where τ_{∞} , T_0 , and D are fitting parameters. As can be seen on Fig. 3b, $\tau_{\alpha}(T)$ dependence of FL + 25 wt% PVAc can be well parameterize by VFT formula with the $\log_{10}(\tau_{\infty}/s)$, T_0 , and D equal to -13.1 ± 1.1 ; 230.3 ± 6.3 and 7.8 ± 1.7 respectively. To cover whole region of relaxation times needed to determine the glass transition temperature related to the α' -process we measured partially re-crystallized sample again. During this, additional measurement the dielectric spectra of the examined sample have been registered on the cooling from $T = 334$ to $T = 290$, with step of 2 K. Points obtained from the analysis of these spectra are marked in Fig. 3b as an open brown circles. As can be seen, now the $\tau_{\alpha'}(T)$ dependence can be properly parameterize by the VFT equation. The values of VFT fit parameters for $\tau_{\alpha'}$ of FL + 25 wt% PVAc are equal to $\log_{10}(\tau_{\infty}/s) = -13.7 \pm 0.3$; $T_0 = 240.5 \pm 2.1$ and $D = 8.5 \pm 0.5$.

From the extrapolation of the VFT fits to $\tau_{\alpha/\alpha'} = 100$ s, we subsequently estimated both the initial, and the final T_g values of the examined drug-polymer system. The initial glass transition temperature was equal to 283 K. This value is in perfect agreement with that obtained from DSC experiment (see Fig. 1). The glass transition temperature determined after sample re-crystallization, i.e. based on α' -process, has a value of 296 K ($T_g = T(\tau_{\alpha/\alpha'} = 100$ s)). To confirm the glass transition temperature of newly obtained concentration of FL + PVAc, we collected the sample after BDS experiment, and additionally measured it via DSC technique. Obtained by different experimental technique T_g was equal to 300 K. To exclude the possibility that whole amount of FL re-crystallized from the investigated ASD, we additionally compare obtained T_g value to the glass transition temperature of neat PVAc polymer. Accordingly to DSC data PVAc has $T_g = 314$ K (see Fig. 1). Substantial temperature difference between final T_g value of FL + 25 wt% of PVAc and T_g of neat polymer indicates that not entire FL re-crystallized from the investigated system. If only polymeric additive would remain amorphous, the final T_g value would be identical as for PVAc. Nevertheless, there are still three things left to do: first of all on the basis of the determined value of final glass transition temperature, we need to assess what is the concentration of the obtained drug-polymer system; secondly, we need to verify if different than FL + 25 wt% PVAc composition (but also unstable) will also re-crystallize to the same final concentration; thirdly, it should be checked if so-called final concentration is indeed highly physically stable.

Previously determined the polymer concentration dependence of T_g

– presented in Fig. 2 – was used to determine the final drug-polymer concentration that has been obtained during both BDS and DSC measurements. As can be seen, according to the T_g value, the newly obtained concentration of the FL + PVAc mixture contains 65 wt% of the polymer. Because it was not confirmed that each supersaturated FL + PVAc system tend to transform to FL + 65 wt% PVAc concentration, we repeated described above set of experiments on different initial – FL + 6 wt% PVAc – concentration. Results obtained from these studies led us exactly to the same conclusions i.e. this drug-polymer system, similarly to the FL + 25 wt% PVAc, re-crystallize to the final concentration characterized by the glass transition temperature equal to 300 K (confirmed by both BDS, and DSC). This clearly indicates that the excess amount of the API will always re-crystallize from the unstable/supersaturated system to its thermodynamically stable concentration containing 65 wt% of PVAc.

In order to check whether transformed concentration has indeed 65 wt% of PVAc polymer, we: (i) prepared such a binary amorphous drug-polymer ASD; (ii) examined its molecular dynamics by means of BDS, and (iii) compared the obtained results to the data obtained after re-crystallization of the sample containing 25 wt% of PVAc. The representative dielectric loss spectra of FL + 65 wt% of PVAc are presented in Fig. 4a. As can be seen on the spectra recorded above the ASD glass transition temperature one well resolved structural relaxation process can be observed. This mode moves toward higher frequencies with increasing temperature and even up to the melting temperature ($T_m = 368$ K) its intensity does not decrease. This indicates that prepared FL + 65 wt% PVAc system does not reveal tendency towards re-crystallization. From the analysis of the dielectric loss spectra collected at $T > T_g$ we were able to determine the temperature dependence of structural relaxation times of FL + 65 wt% PVAc. The $\tau_\alpha(T)$ dependence of this drug-polymer ASD is presented as brown circles on Fig. 4b. Comparing it to the $\tau_\alpha(T)$ dependence of transformed FL + 25 wt% PVAc (see brown stars with black outline in Fig. 4b) one might conclude that both $\tau_\alpha(T)$ of FL + 65 wt% PVAc and $\tau_\alpha(T)$ of partially re-crystallized FL + 25 wt% of PVAc overlap perfectly with each other. This

clearly suggests that transformed sample might indeed contain 65 wt% of PVAc polymer. To parametrize the presented temperature dependence of structural relaxation times of FL + 65 wt% PVAc we employed VFT equation (see Eq. (5)) with the $\log_{10}(\tau_\infty/s)$, T_0 , and D equal to 13.4 ± 0.2 ; 239.9 ± 1.8 and 8.4 ± 0.4 , respectively. From the extrapolation of VFT fit to 100 s we estimated T_g of this composition as 296 ($T_g = T(\tau_\alpha = 100$ s)), what is in perfect agreement with the T_g value of FL + 25 wt% PVAc after transformation. This is another proof that unstable concentrations of investigated drug-polymer system re-crystallize to composition containing 65 wt% of the polymeric additive.

As a final confirmation that unstable compositions of FL + PVAc re-crystallize to concentration containing 65 wt% of the polymer we also compared the shapes of the α -relaxation peak of FL + 65 wt% PVAc, and α' -relaxation peak of FL + 25 wt% PVAc, which were recorded at the same temperature – see Fig. 4c. As can be seen, besides dc-conductivity both compared processes overlap perfectly with each other. This might be taken as evidence that after transformation the unstable FL + 25 wt% PVAc concentration convert to other system containing 65 wt% of the polymer. This consequently means that 65 wt% of PVAc is the lowest polymer amount which is able to fully stabilize amorphous FL. It is worth to recall the results where different polymer – Kollidon VA64 – has been used to improve stability of FL. In that case, to achieve analogous result – physically stable amorphous FL – we had to use 41 wt% of polymer addition [34]. Comparison of these results implies that PVAc is weaker stabilizer of amorphous FL than Kollidon VA64. Accordingly in the next section the evaluation of the remaining component of the co-polymer will be examined in order to verify whether or not the PVP is a greater stabilizer of amorphous FL than PVAc or even Kollidon VA64.

3.3. Thermal properties of FL + PVP mixtures

Thermal properties of neat PVP and the following FL + PVP ASDs: FL + 7 wt% PVP, FL + 15 wt% PVP, FL + 29 wt% PVP, FL + 40 wt% PVP, FL + 60 wt% PVP and FL + 80 wt% PVP have been measured using DSC technique. During these studies all samples (besides neat polymer) were heated up in the same temperature range, from 260 K to 410 K, with the standard heating rate of 10 K/min. The neat PVP polymer was heated up to higher, than in case of other samples, temperature equal to 570 K with the same rate equal to 10 K/min. Results of these studies were compared with DSC thermogram of neat API and are presented in Fig. 5. As can be seen, with increasing amount of polymeric excipient, value of glass transition temperature of the binary drug-polymer system increases.

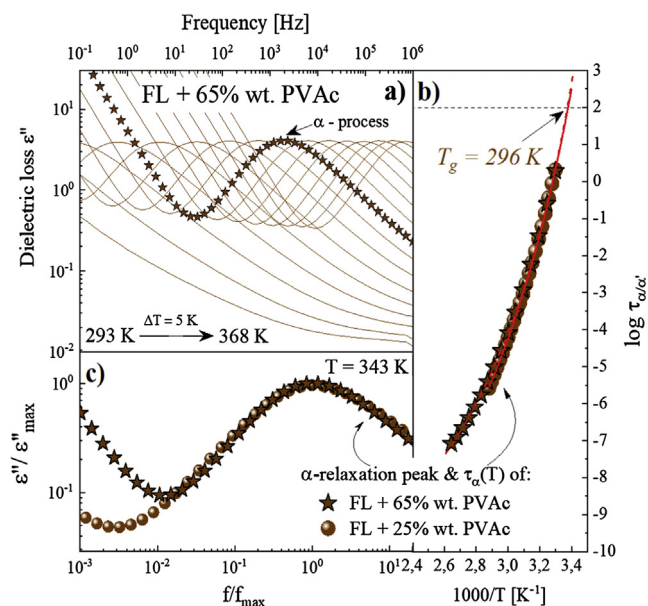


Fig. 4. Dielectric loss spectra of amorphous binary mixture of FL + 25 wt% PVAc (a). Temperature dependence of τ_α for FL + 65 wt% PVAc (brown stars) and FL + 25 wt% PVAc (brown circles) after crystallization in the super cooled liquid has been described by VFT equation (red solid line) (b). Masterplot of two dielectric spectra obtained in the same temperature $T = 343$ K for both FL + 65 wt% PVAc (brown stars) and FL + 25 wt% PVAc after crystallization (brown circles) (c). (For interpretation of the references to colour in this figure legend, the reader is referred to the web version of this article.)

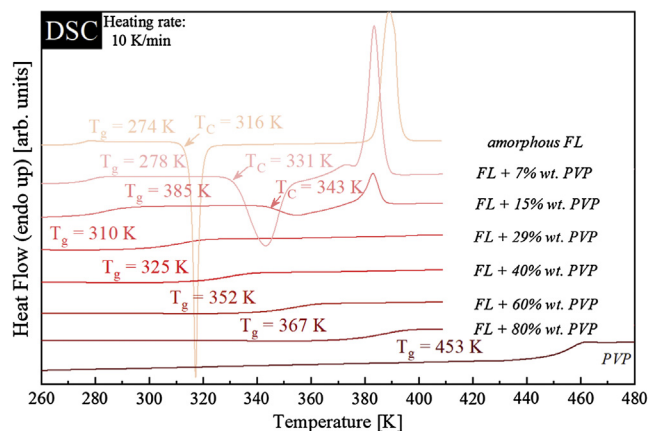


Fig. 5. Thermograms of amorphous: FL (peach), FL + 7 wt% PVP (pink), FL + 15 wt% PVP (salmon), FL + 29 wt% PVP (raspberry), FL + 40 wt% PVP (red), FL + 60 wt% PVP (cardinal), FL + 80 wt% PVP (carmine) and PVP (wine). (For interpretation of the references to colour in this figure legend, the reader is referred to the web version of this article.)

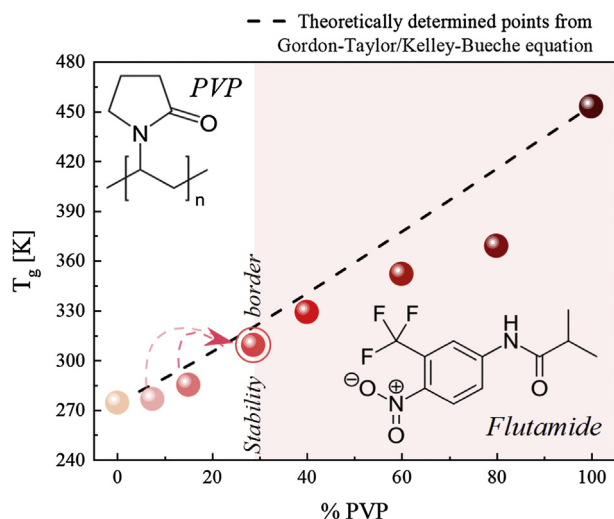


Fig. 6. Glass transition temperatures of FL – PVP mixtures. Points correspond to the experimentally determined T_g values. The dashed line represents the Gordon-Taylor/Kelley-Bueche equation. Ring is the value obtained by using T_g related to the $\tau_{\alpha'}$ process (T_g obtain when crystallization ceased).

The T_g values of investigated samples are equal to: 274 K, 278 K, 285 K, 310 K, 328 K, 352 K, 367 K, 453 K for 0, 7, 15, 29, 40, 60, 80 and 100 wt% of PVP polymer, respectively. To check whether in case of the investigated in this part of the paper systems the antiplasticization effect is dominant reason of increasing T_g value with the polymer content – similarly to FL + PVAc case – we compared the experimentally obtained T_g s of the mixtures with the T_g values predicted from the GT equation (see Fig. 6). As can be seen experimental points deviate from the GT prediction, indicating that some drug-polymer interactions might occur between FL and PVP. It is worth noting that similar pattern of behavior has been previously reported for many different binary PVP-based systems (for example: Bendroflumethiazide-PVP; Hydroflumethiazide-PVP; Hydrochlorothiazide-PVP and Sucrose-PVP [40,41]). In all recalled cases, the deviation of experimentally obtained T_g s from that predicted, based on GT equation, was indeed connected with drug-polymer interactions. This clearly suggests that PVP polymer has a huge tendency to interact with a drugs dispersed in it [42].

Referring back to the Fig. 5, one might observed that only FL + 7 wt% PVP and FL + 15 wt% PVP among all examined ASDs reveal re-crystallization tendency when heated up above T_g with the rate equal to 10 K/min. The onsets of the exothermic crystallization peaks were found to be 331 K and 343 K for FL + 7 wt% PVP and FL + 15 wt% PVP, respectively. It should be noted, that lack of the re-crystallization in case of other drug-polymer concentrations does not guarantee that they will be physically stable also during different experiments, when different conditions e.g. slower heating rate, will be employed. To assess border – physically stable – drug-polymer concentration in case of the FL + PVP ASD, the dielectric studies were performed. Results from these studies are presented and discussed in the next section. Initial concentration, which has been chosen for these experiments, contained 7 wt% of PVP. The reason of this particular choice was caused by the fact, that this drug-polymer concentration revealed crystallization tendencies during DSC studies. If the crystallization process would not occur the observation of the changes in concentration would be impossible.

3.4. Molecular dynamics studies of FL-PVP mixtures

Representative dielectric loss spectra of FL + 7 wt% of PVP polymer are presented in Fig. 7a. Analogously, as for a FL + PVAc systems the spectra collected at $T < T_g$ show absence of any secondary relaxation processes thus revealing NCL. Above the glass transition temperature

the dielectric loss spectra of FL + 7 wt% PVP exhibit structural – α – relaxation process which moves toward higher frequencies with increasing temperature. Its intensity remains unchanged up to the 306 K. Further increasing of the temperature results in the decrease of intensity of the α -relaxation peak, what is a manifestation of the sample re-crystallization. As can be seen in Fig. 7a devitrification process ceases at a temperature equal to 338 K – no further drop of the α -relaxation peak intensity was observed. In Fig. 7c we presented the arbitrary chosen dielectric loss spectrum of FL + 7 wt% PVP, which was recorded just remaining after observed re-crystallization of a part of the volume i.e. at $T = 343$ K. As can be seen the displayed spectrum exhibit three features: dc conductivity associated with translational motion of ions as well as two loss peaks. High contribution of dc conductivity to the dielectric loss spectra, during BDS measurements was already reported in cases of celecoxib and bicalutamide mixtures containing PVP [25,43]. Peak with maximum at higher frequencies represent structural – α' – relaxation process of newly formed drug-polymer concentration. We suppose that peak located at lower frequency side reflects the γ -relaxation of PVP polymer. This would be consistent with the data reported for the secondary relaxation process in neat polymer [44]. It should be noted that the presence of an additional relaxation process set at low frequency side of the structural relaxation was also observed in case of bicalutamide-PVP system [45]. In recalled example, it was found, that this additional process is in fact secondary relaxation process originating from a neat polymer.

Dielectric loss spectra of fully amorphous FL + 7 wt% PVP, which have been registered above the glass transition temperature, were fitted in similar way like in case of FL + PVAc mixtures i.e. by means of single HN function (see Eq. (3)). While the spectra of partially re-crystallized sample, due to presence of more than one loss peak, were analyzed by fitting a sum of HN functions as follow:

$$\varepsilon^*(\omega) = \varepsilon_{\infty} + \sum_k \frac{\Delta\varepsilon_k}{[1 + (i\omega\tau_{HNk})^a]^b} \quad (6)$$

where k is sums over the different relaxation processes, ε_{∞} is high frequency limit permittivity of the real part $\varepsilon'(\omega)$, $\Delta\varepsilon$ is dielectric strength of the process under investigation, ω is the angular frequency $\omega = 2\pi f$, τ_{HN} is the HN relaxation time, which is related to the frequency of maximum loss f_{max} , a and b represents symmetric and asymmetric broadening of relaxation peak. Moreover, DC conductivity effects were taken into account by adding a contribution ($\sigma_{DC}/\varepsilon_0\omega$) to the imaginary part of the fit function. ε_0 is the permittivity of vacuum, while σ_{DC} is the dc conductivity of the sample.

From fitting parameters we calculated, according to Eq. (4), the relaxation times of: structural relaxation of fully amorphous sample (τ_{α}), structural relaxation of partially re-crystallized sample ($\tau_{\alpha'}$), as well as secondary γ relaxation, which is visible on the spectra of partially re-crystallized sample. However, due to the high DC contribution additional analysis based on the derivative formalism according to the following formula [45,46] was required:

$$\varepsilon_{der} = -\frac{\pi d\varepsilon'(f)}{2 d \ln f} \quad (7)$$

This procedure allowed us to eliminate the dc contribution and made the relaxation processes narrower and as a consequence easier to fit (Fig. 7c, blue solid line). As can be seen in Fig. 7c, maxima of the ε_{der} peaks corresponds with the results of fitting by sum of HN functions (Fig. 7c, γ and α' process) which confirms our assumption. Due to the fact that our aim is to determinate the physically stable concentration of FL + PVP system, in the following discussion we will concentrate only on structural (α and α') relaxation processes. In Fig. 7b one can see the temperature dependences of both τ_{α} and $\tau_{\alpha'}$ marked as filled orange and red circles, respectively. Similarly to the case of FL + PVAc we measured partially re-crystallized FL + 7 wt% PVP again. During this, additional experiment the dielectric spectra were examined on the cooling

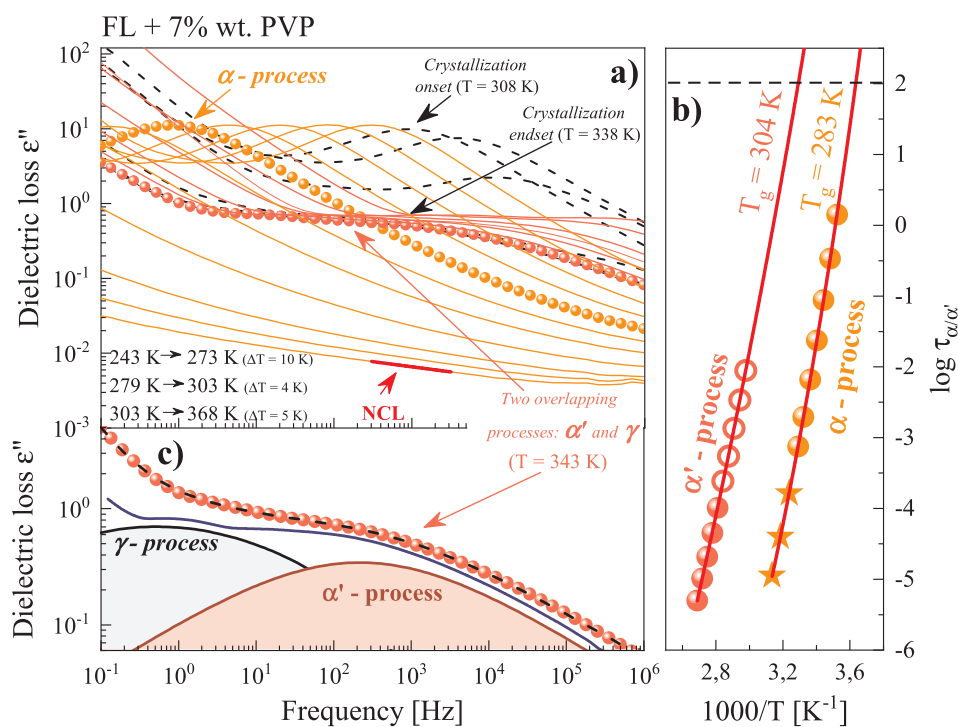


Fig. 7. Dielectric loss spectra of FL + 7 wt% PVP orange circles represents α -relaxation process, black dashed line corresponds to the crystallization process, red circles represents superposition of the α' -process of the newly formed concentration with the γ -process of the neat polymer (a). Right panel shows relaxation map of binary mixtures of FL + 7 wt% PVP as follows: τ_{α} (orange circles), crystallization of FL + 7 wt% PVP (orange stars), τ_{α} (red circles) and $\tau_{\alpha'}$ obtained during cooling (red open circles). Temperature dependence of τ_{α} and $\tau_{\alpha'}$ in the supercooled liquid has been described by VFT equations (red solid lines) (b). Dielectric loss spectrum of FL + 7 wt% PVP registered at 343 K (red circles), fit of sum of the HN function (dashed line), secondary relaxation process of the neat polymer (black solid line) and primary relaxation process of measured system after crystallization (red solid line), spectrum analyzed with derivative method (blue solid line) (c). (For interpretation of the references to colour in this figure legend, the reader is referred to the web version of this article.)

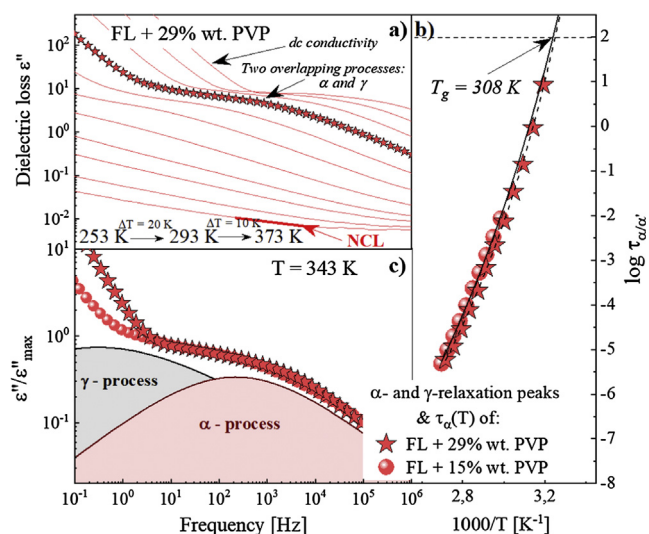


Fig. 8. Dielectric loss spectra of FL + 29 wt% PVP, red line corresponds to the NCL while the red stars to the relaxation process (a). Temperature dependence of FL + 29 wt% PVP τ_{α} (red stars) as well as FL + 7 wt% PVP $\tau_{\alpha'}$ (red circles) in the supercooled liquid has been described by VFT equations (black solid lines) (b). Dielectric loss spectra of FL + 7 wt% PVP (red circles) and FL + 29 wt% PVP (red stars) registered at 343 K, secondary relaxation process of the neat polymer (black solid line) and primary relaxation process of measured system after crystallization (red solid line) (c). (For interpretation of the references to colour in this figure legend, the reader is referred to the web version of this article.)

from $T = 371$ K to $T = 295$ K, with step of 4 K. Data points obtained from analysis of these newly registered spectra are marked in Fig. 7b as an open red circles. In the next step both $\tau_{\alpha}(T)$ and $\tau_{\alpha'}(T)$ dependences were parametrize by the VFT equations. The values of VFT fits parameters are equal to: $\log_{10}(\tau_{\infty}/s) = -14.2 \pm 0.4$; $T_0 = 232.9 \pm 2.9$; $D = 11.9 \pm 1.8$ and $\log_{10}(\tau_{\infty}/s) = 16.1 \pm 1.8$; $T_0 = 216.1 \pm 19.5$ and $D = 17.8 \pm 6.8$ for $\tau_{\alpha}(T)$ and $\tau_{\alpha'}(T)$, respectively. From the extrapolation of these VFT fits to $\tau_{\alpha}/\alpha' = 100$ s, we estimated the initial

and the final T_g values of the examined drug-polymer ASD. The glass transition temperature corresponding to the initial, i.e. FL + 7 wt% of PVP, drug-polymer concentration is equal to 275 K. It is worth noting that this value is in good agreement with T_g obtained from the DSC (see Fig. 5). The value of glass transition temperature determined from the data obtained after the re-crystallization of the excess amount of the drug, is equal to 308 K. Like in case of FL + PVAc, in order to determine this T_g value, we collected the sample after BDS experiment, and examined it via DSC technique. Obtained in this way, value of glass transition temperature of newly achieved concentration of FL + PVAc is in good agreement with T_g calculated based on BDS experiment ($T_{gDSC} = 312$ K). Taking into account that in case of FL + PVP ASDs, we observed deviation of the experimentally determined T_g values from the GT prediction we cannot use the GT prediction to obtain the final drug-polymer concentration. Therefore, to do that, we had to rely on experimentally determined concentration dependence of T_g presented in Fig. 6 as a black dashed line. Comparing T_g value of the newly obtained drug-polymer composition to aforementioned concentration dependence of T_g , it can be clearly seen, that new system should have approximately 29 wt% of PVP polymer content (see open circle on Fig. 6).

To confirm that unstable concentrations of FL + PVP system indeed tends to reach the physically stable concentration containing 29 wt% of the polymer we: (i) prepared different initial – FL + 15 wt% PVP – concentration, which according to DSC data also easily re-crystallizes, and we studied it by similar methods as FL + 7 wt% PVP; (ii) prepared ASD containing FL and exactly 29 wt% of PVP, measured it and finally compare results to data obtained from the evaluation of the transformed FL + 7 wt% PVP. Results obtained from these first experiments (not presented due to many similarities to FL + 7 wt% PVP) indicate that different than 7 wt% of PVP polymer concentration of FL-based ASD (with crystallization tendencies) also transforms to different than initial, but having T_g at 308 K drug-polymer composition. Dielectric loss spectra of potentially stable concentration of FL and PVP (FL + 29 wt% PVP) are presented in Fig. 8a. As can be seen on the spectra collected at $T > T_g$ three main features can be distinguished: dc conductivity, and two poorly separated from each other loss peaks. It is worth to recall that the spectra of partially re-crystallized FL + 7 wt% of PVP ASD exhibit the same main features. To compare the shapes of spectra of

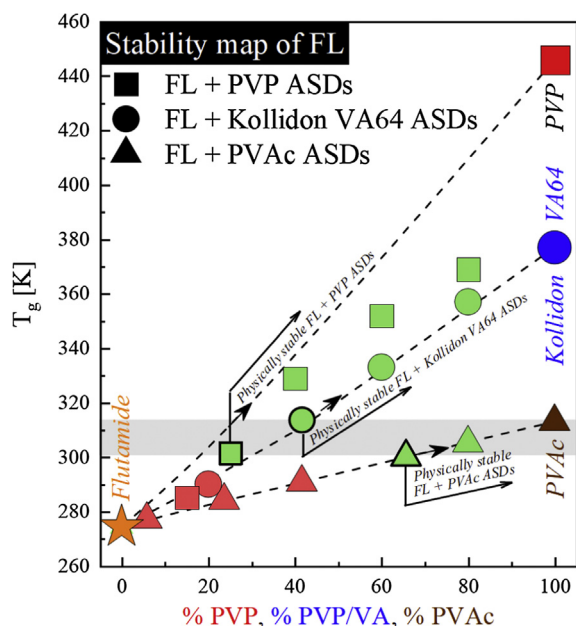


Fig. 9. Stability map obtained for 3 different FL-based ASDs. Star is assigned to the neat amorphous flutamide, and the square, circle and triangle indicates the PVP, PVP/VA and PVAc respectively. GT prediction was marked as a black dashed line. Outlined shapes indicates the concentration obtained after re-crystallization process.

FL + 29 wt% PVP and partially re-crystallize FL + 7 wt% PVP we plotted their representatives (both collected at $T = 343$ K) together in Fig. 8c. Visible similarity is the first suggestion that unstable FL + PVP ASDs indeed transform to FL-based mixture having 29 wt% of the polymer. Since on the dielectric spectra, presented in Fig. 8a, two relaxation processes can be noted we analyzed them by fitting a sum of HN functions (Eq. (6)). On the basis of the estimated from the fitting procedure values of τ_{HN} , a and b, we determined the temperature dependence of τ_{α} (see red circles in Fig. 8b). To parameterize this dependence we fitted the data by VFT equation (Eq. (5)). From the extrapolation of the fit to 100 s we subsequently estimated the glass transition temperature of the investigated system as $T_g = 308$ K. Comparison of both: $\tau_{\alpha}(T)$ of FL + 29 wt% PVP to $\tau_{\alpha}(T)$ of FL + 7 wt% PVP (see Fig. 8b), and T_g value of FL + 29 wt% PVP to T_g value of partially re-crystallize FL + 7 wt% PVP indicate that both these samples have a lot in common. Consequently one can conclude that minimal amount of PVP which is indeed required to fully stabilize amorphous form of FL is equal to 29 wt% of the polymer.

3.5. Comparison of the stabilization effect of three different polymers on amorphous FL

From all performed experiments and analysis, we were able to obtain the “stability map” presenting concentration dependence of glass transition temperature of FL + PVAc and FL + PVP compositions (see Fig. 9). Because similar dependence had been recently determined by us for other FL-based ASDs (containing co-polymer made of PVAc and PVP i.e. Kollidon VA64), we also plotted these data in the same graph to compare the effect of FL stabilization by all three polymers. As can be seen, the concentration needed to stabilize amorphous FL varies from each investigated excipient. The minimal amount of PVAc polymer that is required to obtain physically stable FL-based ASD is equal to 65 wt%. To stabilize the examined antiandrogen by PVP, we need to use at least 29 wt% of this polymer. While, as Fig. 9 presents, the required amount of Kollidon VA64 that can eliminate FL re-crystallization is equivalent to 41 wt%. Moreover, it is worth to mention that described high physical stability of FL-PVP/VA system, prepared in this way, has been

confirmed by means of long-term XRD measurements. Evaluated sample did not exhibit any tendency towards crystallization, during long-term stability studies measured at room temperature for over 450 days (up to date). Taking these numbers into account we might conclude that PVP is the best stabilizer of FL, while the PVAc shows the weakest stabilizing effect on this API. Based on presented results we might ranked polymers from the better FL’s stabilizer in the following order PVP > Kollidon VA64 > PVAc. Interestingly, the greater T_g value of polymer, the lower the concentration of excipient is needed to stabilize FL.

4. Conclusions

In this article we employed two different polymers: PVP and PVAc to improve the physical stability of the amorphous form of FL. Prepared drug-polymer compositions containing various amount of polymeric additive were investigated by means of differential scanning calorimetry as well as broadband dielectric spectroscopy. We found that both polymers can effectively inhibit re-crystallization of the investigated antiandrogen. Lack of deviation of experimentally obtained concentration dependence of T_g value from the GT prediction suggests that in case of FL + PVAc mixtures the antiplasticization effect is the main reason of FL stabilization. Probably the opposite situation exists in case of FL + PVP ASDs i.e. presence of deviation of experimentally obtained T_g values from GT predictions suggests that between drug and polymer might occur some interactions. Due to the fact that during non-isothermal dielectric measurements of both: FL + PVAc and FL + PVP systems, the transformation from supersaturated to saturated ASDs could be registered, we were able to determine the border – drug-polymer – concentration, which guarantee high physical stability of the investigated systems. According to our analysis the minimal amount of the polymeric excipient, which is required to fully stabilize FL drug is equal to: 65 wt% and 29 wt% of PVAc and PVP, respectively. These results clearly indicate that PVP polymer is much better stabilizer of the investigated antiandrogen than PVAc. Another word, to fully stabilize FL we need definitely less PVP than PVAc. Because, PVP and PVAc polymers are a components of co-polymer Kollidon VA64, we compared obtained in this paper results to already published data. This comparison confirmed our expectations that the system made of PVP and PVAc has intermediate, in comparison to its individual parts, effect on stabilization improvement of FL. To fully stabilize FL by Kollidon VA64 we need 41 wt% of the excipient.

Acknowledgement

The authors, K.C., and M.P., are grateful for the financial support received within the Project No. 2015/16/W/NZ7/00404 (SYMFONIA 3) from the National Science Centre, Poland. Moreover, J.K-K. thank FNP for awarding grants within the framework of the START Program (2017).

References

- [1] D. Singhal, W. Curatolo, Drug polymorphism and dosage form design: a practical perspective, *Adv. Drug Deliv. Rev.* 56 (2004) 335–347, <https://doi.org/10.1016/j.addr.2003.10.008>.
- [2] C. Bhugra, M.J. Pikal, Role of thermodynamic, molecular, and kinetic factors in crystallization from the amorphous state, *J. Pharm. Sci.* 97 (2008) 1329–1349, <https://doi.org/10.1002/jps.21138>.
- [3] J. Tao, Y. Sun, G.G.Z. Zhang, L. Yu, Solubility of small-molecule crystals in polymers: D-Mannitol in PVP, indomethacin in PVP/VA, and nifedipine in PVP/VA, *Pharm. Res.* 26 (2009) 855–864, <https://doi.org/10.1007/s11095-008-9784-z>.
- [4] N.J. Babu, A. Nangia, Solubility advantage of amorphous drugs and pharmaceutical cocrystals, *Cryst. Growth Des.* 11 (2011) 2662–2679, <https://doi.org/10.1021/cg200492w>.
- [5] Y. Tian, V. Caron, D.S. Jones, A.M. Healy, G.P. Andrews, Using Flory-Huggins phase diagrams as a pre-formulation tool for the production of amorphous solid dispersions: a comparison between hot-melt extrusion and spray drying, *J. Pharm. Pharmacol.* 66 (2014) 256–274, <https://doi.org/10.1111/jphp.12141>.

- [6] C. Leuner, J. Dressman, Improving drug solubility for oral delivery using solid dispersions, *Eur. J. Pharm. Biopharm.* 50 (2000) 47–60, [https://doi.org/10.1016/S0939-6411\(00\)00076-X](https://doi.org/10.1016/S0939-6411(00)00076-X).
- [7] T. Vasconcelos, B. Sarmento, P. Costa, Solid dispersions as strategy to improve oral bioavailability of poor water soluble drugs, *Drug Discov. Today* 12 (2007) 1068–1075, <https://doi.org/10.1016/j.drudis.2007.09.005>.
- [8] B.C. Hancock, M. Parks, What is the true solubility advantage for amorphous pharmaceuticals? *Pharm. Res.* 17 (2000) 397–404, <https://doi.org/10.1023/A:1007516718048>.
- [9] J. Knapik, Z. Wojnarowska, K. Grzybowska, K. Jurkiewicz, L. Tajber, M. Paluch, Molecular dynamics and physical stability of coamorphous ezetimib and indapamide mixtures, *Mol. Pharm.* 12 (2015) 3610–3619, <https://doi.org/10.1021/acs.molpharmaceut.5b00334>.
- [10] S.P. Bhardwaj, R. Suryanarayanan, Molecular mobility as an effective predictor of the physical stability of amorphous trehalose, *Mol. Pharm.* 9 (2012) 3209–3217, <https://doi.org/10.1021/mp300302g>.
- [11] a. Forster, J. Hemenstall, T. Rades, Characterization of glass solutions of poorly water-soluble drugs produced by melt extrusion with hydrophilic amorphous polymers, *J. Pharm. Pharmacol.* 53 (2001) 303–315, <https://doi.org/10.1211/0022357011775532>.
- [12] S.B. Murdande, M.J. Pikal, R.M. Shanker, R.H. Bogner, Solubility advantage of amorphous pharmaceuticals: I. A thermodynamic analysis, *J. Pharm. Sci.* 99 (2010) 1254–1264, <https://doi.org/10.1002/jps.21903>.
- [13] R. Paus, Y. Ji, L. Vahle, G. Sadowski, Predicting the solubility advantage of amorphous pharmaceuticals: a novel thermodynamic approach, *Mol. Pharm.* 12 (2015) 2823–2833, <https://doi.org/10.1021/mp500824d>.
- [14] A.T.M. Serajuddin, Solid dispersion of poorly water-soluble drugs: Early promises, subsequent problems, and recent breakthroughs, *J. Pharm. Sci.* 88 (1999) 1058–1066, <https://doi.org/10.1021/js980403l>.
- [15] J. Knapik-Kowalczyk, Z. Wojnarowska, K. Chmiel, M. Rams-Baron, L. Tajber, M. Paluch, Can Storage Time Improve the Physical Stability of Amorphous Pharmaceuticals with Tautomerization Ability Exposed to Compression? The Case of a Chloramphenicol Drug, *Mol. Pharm.* (2018) *acs.molpharmaceut.8b00099*. 10.1021/acs.molpharmaceut.8b00099.
- [16] S.P. Bhardwaj, K.K. Arora, E. Kwong, A. Templeton, S.D. Clas, R. Suryanarayanan, Correlation between molecular mobility and physical stability of amorphous itraconazole, *Mol. Pharm.* 10 (2013) 694–700, <https://doi.org/10.1021/mp300487u>.
- [17] J. Knapik, Z. Wojnarowska, K. Grzybowska, K. Jurkiewicz, A. Stankiewicz, M. Paluch, Stabilization of the amorphous ezetimibe drug by confining its dimension, *Mol. Pharm.* 13 (2016) 1308–1316, <https://doi.org/10.1021/acs.molpharmaceut.5b00903>.
- [18] J. Knapik-Kowalczyk, Z. Wojnarowska, M. Rams-Baron, K. Jurkiewicz, J. Cielecka-Piontek, K.L. Ngai, M. Paluch, Atorvastatin as a promising crystallization inhibitor of amorphous probucol: dielectric studies at ambient and elevated pressure, *Mol. Pharm.* 14 (2017) 2670–2680, <https://doi.org/10.1021/acs.molpharmaceut.7b00152>.
- [19] K. Lehmkemper, S.O. Kyeremateng, M. Bartels, M. Degenhardt, G. Sadowski, Physical stability of API/polymer-blend amorphous solid dispersions, *Eur. J. Pharm. Biopharm.* 124 (2018) 147–157, <https://doi.org/10.1016/J.EJPB.2017.12.002>.
- [20] K. Löbmann, C. Strachan, H. Grohgan, T. Rades, O. Korhonen, R. Laitinen, Co-amorphous simvastatin and glipizide combinations show improved physical stability without evidence of intermolecular interactions, *Eur. J. Pharm. Biopharm.* 81 (2012) 159–169, <https://doi.org/10.1016/j.ejpb.2012.02.004>.
- [21] P.J. Marsac, T. Li, L.S. Taylor, Estimation of drug-polymer miscibility and solubility in amorphous solid dispersions using experimentally determined interaction parameters, *Pharm. Res.* 26 (2009) 139–151, <https://doi.org/10.1007/s11095-008-9721-1>.
- [22] G.P. Andrews, O. Abu-Diak, F. Kusmanto, P. Hornsby, Z. Hui, D.S. Jones, Physicochemical characterization and drug-release properties of celecoxib hot-melt extruded glass solutions, *J. Pharm. Pharmacol.* 62 (2010) 1580–1590, <https://doi.org/10.1111/j.2042-7158.2010.01177.x>.
- [23] E. Karavas, M. Georgarakis, A. Docoslis, D. Bikiaris, Combining SEM, TEM, and micro-Raman techniques to differentiate between the amorphous molecular level dispersions and nanodispersions of a poorly water-soluble drug within a polymer matrix, *Int. J. Pharm.* 340 (2007) 76–83, <https://doi.org/10.1016/j.ijpharm.2007.03.037>.
- [24] P. Mistry, K.K. Amponsah-Efah, R. Suryanarayanan, Rapid assessment of the physical stability of amorphous solid dispersions, *Cryst. Growth Des.* 17 (2017) 2478–2485, <https://doi.org/10.1021/acs.cgd.6b01901>.
- [25] K. Grzybowska, K. Chmiel, J. Knapik-Kowalczyk, A. Grzybowski, K. Jurkiewicz, M. Paluch, Molecular factors governing the liquid and glassy states recrystallization of celecoxib in binary mixtures with excipients of different molecular weights, *Mol. Pharm.* 14 (2017) 1154–1168, <https://doi.org/10.1021/acs.molpharmaceut.6b01056>.
- [26] Y. Aso, S. Yoshioka, S. Kojima, Molecular mobility-based estimation of the crystallization rates of amorphous nifedipine and phenobarbital in poly(vinylpyrrolidone) solid dispersions, *J. Pharm. Sci.* 93 (2004) 384–391, <https://doi.org/10.1002/jps.10526>.
- [27] A.C.F. Rumondor, L.A. Stanford, L.S. Taylor, Effects of polymer type and storage relative humidity on the kinetics of felodipine crystallization from amorphous solid dispersions, *Pharm. Res.* 26 (2009) 2599–2606, <https://doi.org/10.1007/s11095-009-9974-3>.
- [28] A. Mahieu, J.-F. Willart, E. Dugonon, F. Danède, M. Descamps, A new protocol to determine the solubility of drugs into polymer matrices, *Mol. Pharm.* 10 (2013) 560–566, <https://doi.org/10.1021/mp3002254>.
- [29] K. Lehmkemper, S.O. Kyeremateng, M. Degenhardt, G. Sadowski, Influence of low-molecular-weight excipients on the phase behavior of PVPVA64 amorphous solid dispersions, *Pharm. Res.* 35 (2018) 25, <https://doi.org/10.1007/s11095-017-2316-y>.
- [30] M.B. Rask, M.M. Knopp, N.E. Olesen, R. Holm, T. Rades, Influence of PVP/VA copolymer composition on drug-polymer solubility, *Eur. J. Pharm. Sci.* 85 (2016) 10–17, <https://doi.org/10.1016/J.EJPS.2016.01.026>.
- [31] M.B. Rask, M.M. Knopp, N.E. Olesen, R. Holm, T. Rades, Comparison of two DSC-based methods to predict drug-polymer solubility, *Int. J. Pharm.* 540 (2018) 98–105, <https://doi.org/10.1016/J.IJPHARM.2018.02.002>.
- [32] S. Li, Y. Tian, D.S. Jones, G.P. Andrews, Optimising drug solubilisation in amorphous polymer dispersions: rational selection of hot-melt extrusion processing parameters, *AAPS PharmSciTech.* 17 (2016) 200–213, <https://doi.org/10.1208/s12249-015-0450-6>.
- [33] Y. Sun, J. Tao, G.G.Z. Zhang, L. Yu, Solubilities of crystalline drugs in polymers: an improved analytical method and comparison of solubilities of indomethacin and nifedipine in PVP, PVP/VA, and PVAc, *J. Pharm. Sci.* 99 (2010) 4023–4031, <https://doi.org/10.1002/jps.22251>.
- [34] K. Chmiel, J. Knapik-Kowalczyk, K. Jurkiewicz, W. Sawicki, R. Jachowicz, M. Paluch, A new method to identify physically stable concentration of amorphous solid dispersions (I): case of flutamide + kollidon VA64, *Mol. Pharm.* 14 (2017) 3370–3380, <https://doi.org/10.1021/acs.molpharmaceut.7b00382>.
- [35] M. Rams-Baron, Z. Wojnarowska, K. Grzybowska, M. Dulski, J. Knapik, K. Jurkiewicz, W. Smolka, W. Sawicki, A. Ratuszna, M. Paluch, Toward a better understanding of the physical stability of amorphous anti-inflammatory agents: the roles of molecular mobility and molecular interaction patterns, *Mol. Pharm.* 12 (2015) 3628–3638, <https://doi.org/10.1021/acs.molpharmaceut.5b00351>.
- [36] F. Kremer, A. Schönhal, Broadband Dielectric Spectroscopy, 2003. <http://doi.org/10.1007/978-3-642-56120-7>.
- [37] H. Vogel, Temperaturabhängigkeitgesetz der Viskosität von Flüssigkeiten, *J. Phys. Z.* (1921) 645–646 (accessed October 3, 2017).
- [38] G.S. Fulcher, Analysis of recent measurements of the viscosity of glasses, *J. Am. Ceram. Soc.* 8 (1925) 339–355, <https://doi.org/10.1111/j.1151-2916.1925.tb16731.x>.
- [39] G. Tammann, W. Hesse, Die Abhängigkeit der Viskosität von der Temperatur bei unterkühlten Flüssigkeiten, *Zeitschrift Für Anorg. Und Allg. Chemie.* 156 (1926) 245–257, <https://doi.org/10.1002/zaac.19261560121>.
- [40] L. Tajber, O.I. Corrigan, A.M. Healy, Physicochemical evaluation of PVP-thiazide diuretic interactions in co-spray-dried composites - Analysis of glass transition composition relationships, *Eur. J. Pharm. Sci.* 24 (2005) 553–563, <https://doi.org/10.1016/j.ejps.2005.01.007>.
- [41] S.L. Shamblin, L.S. Taylor, G. Zografi, Mixing behavior of colyophilized binary systems, *J. Pharm. Sci.* 87 (1998) 694–701, <https://doi.org/10.1021/JS9704801>.
- [42] S. Baghel, H. Cathcart, N.J. O'Reilly, Polymeric amorphous solid dispersions: a review of amorphization, crystallization, stabilization, solid-state characterization, and aqueous solubilization of biopharmaceutical classification system class II drugs, *J. Pharm. Sci.* 105 (2016) 2527–2544, <https://doi.org/10.1016/j.xphs.2015.10.008>.
- [43] J. Szczurek, M. Rams-Baron, J. Knapik-Kowalczyk, A. Antosik, J. Szafraniec, W. Jamróz, M. Dulski, R. Jachowicz, M. Paluch, Molecular dynamics, recrystallization behavior, and water solubility of the amorphous anticancer agent bicalutamide and its polyvinylpyrrolidone mixtures, *Mol. Pharm.* 14 (2017) 1071–1081, <https://doi.org/10.1021/acs.molpharmaceut.6b01007>.
- [44] S. Cerveny, Á. Alegria, J. Colmenero, Broadband dielectric investigation on poly(vinyl pyrrolidone) and its water mixtures, *J. Chem. Phys.* 128 (2008) 044901, <https://doi.org/10.1063/1.2822332>.
- [45] J. Pacuť, M. Rams-Baron, B. Chrzaszcz, R. Jachowicz, M. Paluch, Effect of polymer chain length on the physical stability of amorphous drug-polymer blends at ambient pressure, *Mol. Pharm.* 15 (2018) 2807–2815, <https://doi.org/10.1021/acs.molpharmaceut.8b00312>.
- [46] M. Wübbenhorst, J. Van Turnhout, Analysis of complex dielectric spectra. I: One-dimensional derivative techniques and three-dimensional modelling, *J. Non. Cryst. Solids* (2002) 40–49, [https://doi.org/10.1016/S0022-3093\(02\)01086-4](https://doi.org/10.1016/S0022-3093(02)01086-4).